ASME 2012 Fluids Engineering Summer Meeting
July 8-12, 2012, Puerto Rico, USA

FEDSM2012-72014

SIMULATION AND COMPARISON OF PARTICLE INJECTION IN AN INDOOR ENVIRONMENT USING THE SPECIES TRANSPORT AND DISCRETE PHASE MODELS

Z. C. Zheng
University of Kansas
Lawrence, KS, USA

Z. Wei
University of Kansas
Lawrence, KS, USA

J.S. Bennett
National Institute for Occupational Safety and Health
Centers for Disease Control and Prevention
Cincinnati, OH, USA

X. Yang
Pacific Northwest National Laboratory
Richland, WA, USA

NOMENCLATURE

ρ	=	density, kg/m^3
Y_i	=	local mass fraction of each species
$\mathbf{u}$	=	velocity vector of flow field, m/s
$\mathbf{u_p}$	=	velocity vector of particles, m/s
$D_{i,m}$	=	diffusion coefficient of each species, m^2/s
μ_t	=	turbulent viscosity of flow field, kg/m-s
μ	=	laminar viscosity of flow field, kg/m-s
Sc_t	=	turbulent Schmidt number
$\mathbf{F_D}$	=	the drag force per unit particle mass, m/s^2
C_D	=	the drag coefficient of particles
$\mathbf{F_b}$	=	the additional acceleration term of the DPM Model, force per unit particle mass, m/s^2
$\mathbf{g}$	=	the gravitational force, m/s^2

ABSTRACT

In simulating fluid/solid-particle multiphase -flows, various methods are available. One approach is the combined Euler-Lagrange method, which simulates the fluid phase flow in the Eulerian framework and the discrete phase (particle) motion in the Lagrangian framework simultaneously. The Lagrangian approach, where particle motion is determined by the current state of the fluid phase flow, is also called the discrete phase model (DPM), in the context of numerical flow simulation. In this method, the influence of the particle motions on the fluid flow can be included (two-way interactions) but are more commonly excluded (one-way interactions, when the discrete phase concentration is dilute. The other approach is to treat the particle number concentration as a continuous species, a necessarily passive quantity determined by the fluid flow, with no influences from the particles on the fluid flow (one-way interactions only), except to the extent the discrete phase "continuum" alters the overall fluid properties, such as density. In this paper, we compare these two methods with experimental data for an indoor environmental chamber. The effects of injection particle numbers and the related boundary conditions are investigated. In the Euler-Lagrange interaction or DPM model for incompressible flow, the Eulerian continuous phase is governed by the Reynolds-averaged N-S (RANS) equations. The motions of particles are governed by Newton's second law. The effects of particle motions are communicated to the continuous phase through a force term in the RANS equations. The second formulation is a pure Eulerian type, where only the particle-number concentration is addressed, rather than the motion of each individual particle. The fluid flow is governed by the same RANS equations without the particle force term. The particle-number concentration is simulated by a species transport equation. Comparisons among the models and with experimental and literature data are presented. Particularly, results with different numbers of released particles in the DPM will be investigated.

INTRODUCTION

When considering air quality and human and animal health, it is important to understand spatial distributions of airborne or deposited particles in an enclosed environment such as a room. Lai [1] did a thorough literature review. The geometry and experimental setup of the current study were designed to reflect a situation where powdered particles are dispersed in a room

and settles. For this purpose, a numerical simulation that uses the basic conservation laws is a powerful tool.

The methods to solve fluid/solid-particle multiphase flow problems can be categorized into two different types of formulations, i.e. Euler-Lagrange interaction model (also called the discrete phase model) and the pure Eulerian or Euler-Euler type model. In the Euler-Euler approach, all phases are computed in the Eulerian framework. Recently, Sun et al. [2] conducted research on liquid droplet distribution in a ventilated room, using both Euler-Euler simulation and experiments. Zhang et al [3] carried out a study with the Euler-Euler method on particle deposition at the bottom surface of a room-scale chamber with particle injection. Lai et al. [4] conducted a study on particle distribution in a two-zone chamber to compare with experimental data. The Euler-Lagrange/discrete-phase method is generally used when the volume fraction of the dispersed secondary phase is low. In this approach, the fluid phase is solved as a continuum by Navier-Stokes equations, while the dispersed phase is calculated by summing the forces on particles and tracking their motions. Furthermore, Zhang and Ahmadi [5] presented a numerical study to validate and compare the performance of the Euler-Euler and Euler-Lagrange methods and then applied these methods to a three-phase flow. Lai and Chen [6] presented a numerical study to validate and compare the performance of the Euler-Euler and Euler-Lagrange method.

The current study implements Euler-Euler and Euler-Lagrange methods using a commercial CFD solver. Because this solver does not count the gravitational force (in a particle sense) in the Euler-Euler method, another model will be introduced following those in Zhang et al [3] and Zhang and Zheng [7]. The effects of number of particles and particle size on the DPM model results are studied, and comparisons among models, experiments, and literature are discussed.

SPECIES TRANSPORT EQUATIONS

When considering all the phases as continuous media, the mass fraction of each species is governed by the convection-diffusion equation. For the i^{th} species, the conservation equation, Eq. (1), is computed for the concentration distributions of each species:

$$\frac{\partial}{\partial t}\left(\rho Y_i\right)+\nabla\bullet\left(\rho\mathbf{u}Y_i\right)=\nabla\bullet\left[\left(\rho D_{i,m}+\frac{\mu_t}{\mathrm{Sc_t}}\right)\nabla Y_i\right] \quad (1)$$

Here, ρ is the density of the mixture of all species, and Sc_t is the turbulent Schmidt number related to turbulent diffusivity and is selected as 0.7. Turbulent diffusion generally overwhelms laminar diffusion. Since the mass fractions of the species must sum to unity, Eq. (1) is solved only for the first (N-1) species where N is the total number of continuous phase species in the system.

DISCRETE PHASE MODELING

The fluid phase is still treated as a continuum by solving the Navier-Stokes equations, while the dynamics of particles is calculated by the trajectory method. Exchanges of momentum and energy may exist between the fluid phase and the dispersed phase or particle.

In this model, a fundamental assumption is made that the dispersed phase is of a low volume fraction, practically less than 10-12%, even though higher mass loading can sometimes still be acceptable. The particle trajectories are computed individually based on Newton's second law.

The trajectory of a discrete phase particle is predicted by solving the equation of motion resulting from the various forces acting on each particle, which is written in a Lagrangian reference frame. The equation can be expressed as

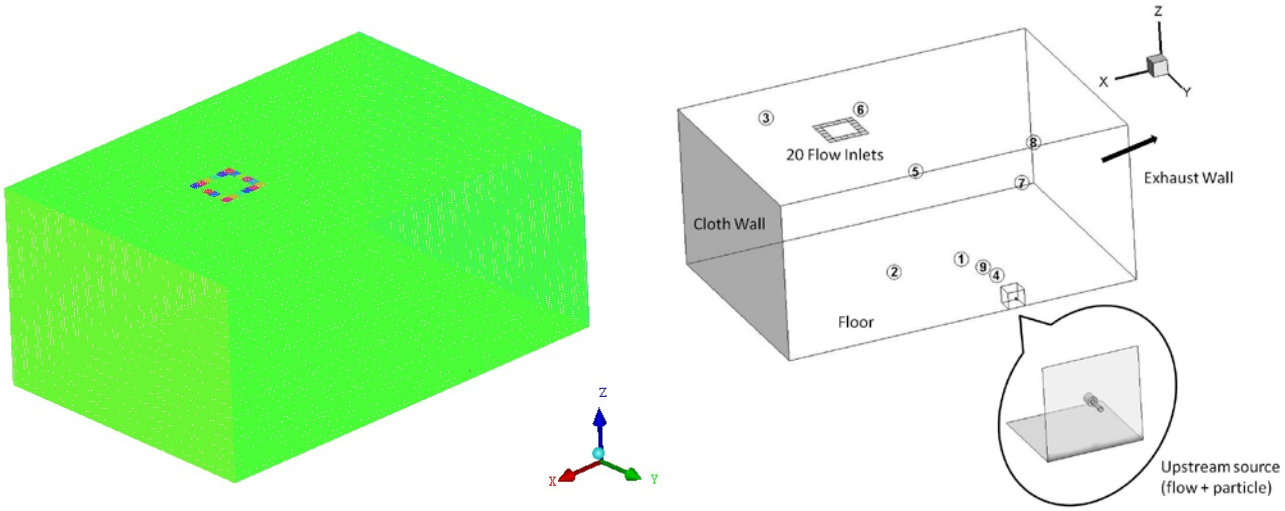

Figure 1- The mesh (left) and the definition sketch of the geometry (right)

$$\frac{d\mathbf{u}_p}{dt} = \mathbf{F_D} + \frac{\mathbf{g}(\rho_p - \rho)}{\rho_p} + \mathbf{F_b} \qquad (2)$$

where $\mathbf{F_D}$ is the drag force per unit particle mass. The drag force is calculated as

$$\mathbf{F_D} = \frac{18\mu}{\rho_p d_p^{\,2}} \frac{C_D \,\mathrm{Re}}{24} (\mathbf{u} - \mathbf{u}_p) \qquad (3)$$

where μ is the molecular viscosity of the fluid, and Re is the relative Reynolds number, defined as

$$\mathrm{Re} \equiv \frac{\rho d_p \left|\mathbf{u_p} - \mathbf{u}\right|}{\mu} \qquad (4)$$

Additional forces, $\mathbf{F}_b$, in the particle force balance may play an important role under special circumstances, i.e. $\rho > \rho_p$. The most important one of them is the "virtual mass" force, which is required to accelerate the fluid surrounding the particle. This force can be written as

$$\mathbf{F_{virtual}} = \frac{1}{2}\frac{\rho}{\rho_p}\frac{d}{dt}\left(\mathbf{u} - \mathbf{u_p}\right) \qquad (5)$$

Moreover, another force is

$$\mathbf{F_{additional}} = \frac{\rho}{\rho_p}\left[\left(\mathbf{u_p} \bullet \nabla\right)\mathbf{u}\right] \qquad (6)$$

In summary, Eq. (7) holds for all simulations in current study.

$$\mathbf{F_b} = \mathbf{F_{virtual}} + \mathbf{F_{additional}} \qquad (7)$$

The drag coefficient, C_D in Eq. (3), has a form for smooth spherical particles used in the current study:

$$C_D = a_1 + \frac{a_2}{\mathrm{Re}} + \frac{a_3}{\mathrm{Re}^2} \qquad (8)$$

where a_1, a_2, and a_3 are constants taken from Morsi and Alexander [8] applying to smooth spherical particles over a wide range of Re. This approach is chosen for its simplicity. Other methods to obtain drag coefficient can be found in Ounis et al [9] and Moshfegh et al [10].

GEOMETRY AND BOUNDARY CONDITIONS

Figure 1 shows the mesh and the sketch of the geometry in the current study. The dimension of this geometry is 5.3848m*3.7084m*2.4384m, with 48.6924 m^3 as the total volume. The velocity inlet consists of 20 small rectangular inlets with different velocity components, which is located at the plane of z = 2.4384m. The gravitational direction is in the positive z-direction. The small rectangle at the bottom left corner is numbered as number one, and the rest small rectangles are assigned numbers in a counter-clockwise manner. The velocity components of each of the small rectangular inlets are listed in Table 1. The area of each small inlet is 0.010322534m^2. According to these boundary conditions, the Reynolds number of each inlet is in the range between 30,000 and 70,000.

The upstream injection source has both flow and particles. Its detailed two-layer shape is drawn at the bottom of the sketch. The center of the circular injection hole is located at (1.855m, 3.708m, 0.133m). Other details on the boundary conditions are listed in Table 2.

Table 1 -- Velocity components of the major flow inlet

Number of inlets	X-Velocity (m/s)	Y-Velocity (m/s)	Z-Velocity (m/s)	Number of inlets	X-Velocity (m/s)	Y-Velocity (m/s)	Z-Velocity (m/s)
1 (bottom left corner)	-4.38	-4.38	-0.25	11 (top right corner)	3.18	3.18	-0.25
2	-5.21	0	-0.25	12	8.2	0	-0.25
3	-4.95	0	-0.25	13	9.97999	0	-0.25
4	-4.86	0	-0.25	14	10.13	0	-0.25
5	-4.966	0	-0.25	15	8.53	0	-0.25
6 (top left corner)	-4.166	4.166	-0.25	16 (bottom right corner)	3.39	-3.39	-0.25
7	0	7.9	-0.25	17	0	-7.75	-0.25
8	0	9.47	-0.25	18	0	-9.75	-0.25
9	0	10.13	-0.25	19	0	-9.6	-0.25
10	0	7.92	-0.25	20	0	-7.95	-0.25

RESULTS AND DISCUSSION

In order to compare the results of the species transport and the DPM model, steady simulations were carried out using the commercial flow solver with a *k-ε* turbulence model. A discussion about differences among turbulence models on prediction of particle deposition can be found in Tian and Ahmadi [11]. Considering the complexity of the geometry, the current study employed a standard *k-ε* model with an increased C_μ value from the standard value of 0.09 to 0.14. This constant was adjusted to match the average variance in the simulated species concentration field to the measured field, by increasing the turbulent viscosity in the simulation. The turbulence model also enables a relatively high order of convergence. The continuous phase simulation is 1^{st}-order accurate in spatial discretization. A simulation without any particle injection (air flow only) was firstly converged to 10^{-4}. A converged flow field before the injection of particles or species can ensure that the cases with either species transport model or the DPM model have an identical, controlled initial condition. In the species transport model, a tracer gas is injected with the same speed of the air flow. The density of the tracer gas (isobutylene) is 2.4 (kg/m^3) and its molecular weight is 56 (kg/kmol). In the DPM model, a single stream injection of water-liquid is applied at the center of the injection hole with -0.035 m/s of y-velocity. The diameter of the particle is set as 1 μm. The total flow rate is 10^{-5} (kg/s), which is computed from the same condition of the species injection. The stochastic tracking for particles in the turbulent flow is employed in the DPM model with 8000 of number of tries. For the steady simulation, this means that 8000 particles are injected and tracked for every DPM computation. A test of number of tries will be discussed later. The experimental results to be compared are from Shulman et al [12].

Table 2- Boundary conditions for all simulations

Boundary	B.C.	Momentum	Turbulence	Species Mass Fraction	DPM
20 Inlets	Inlet	Velocity Components	Turbulence Intensity = 4.1431(%) Turbulence Length Scale = 0.007112(m)	0	escape
Upstream source	Inlet	Velocity Magnitude = 0.035(m/s)	Turbulent Kinetic Energy = 0.01(m^2/s^2) Turbulent Dissipation Rate = 0.01(m^2/s^3)	0.84	escape
Cloth Wall	Wall	Stationary, No slip		0 diffusive flux	reflect
Exhaust Wall	Inlet	Velocity Magnitude = -0.005775(m/s)	Turbulence Intensity = 6.6085(%) Turbulence Length Scale = 0.2(m)	0	escape
Other Walls	Wall	Stationary, No slip		0 diffusive flux	trap

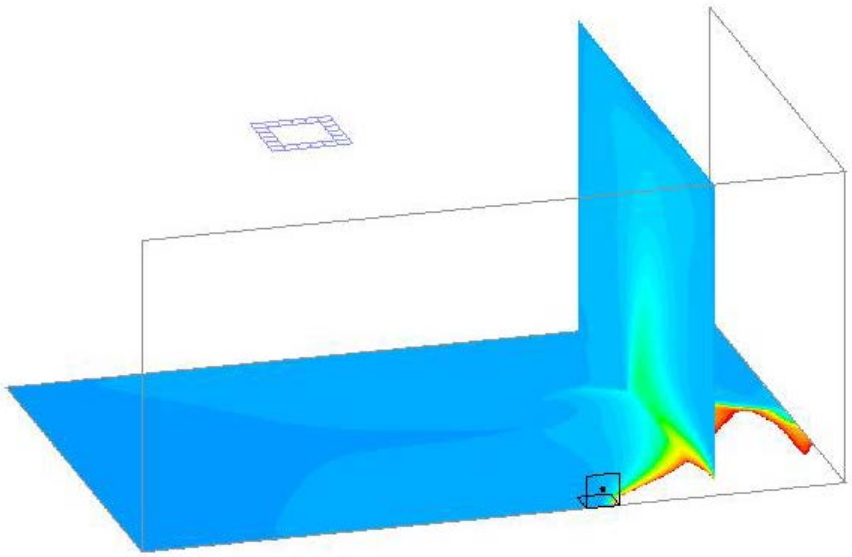

(a)

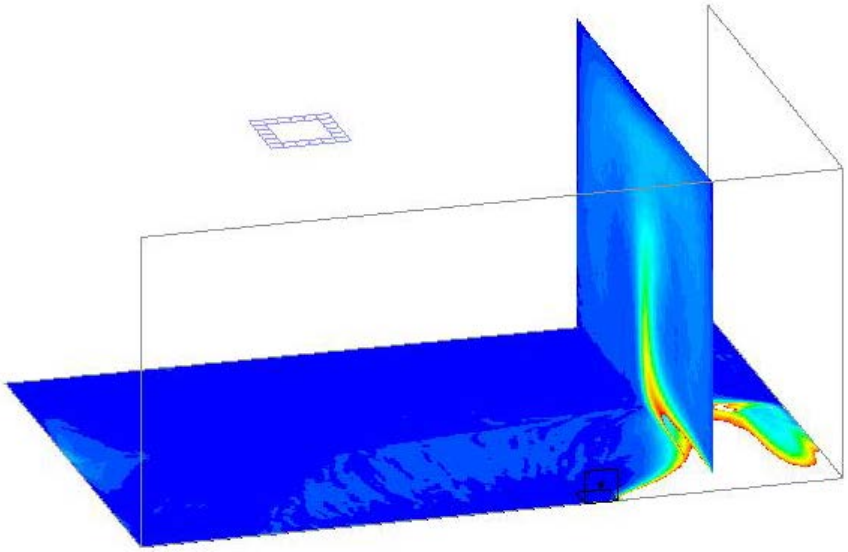

(b)

Figure 2 - Comparisons of particle mole concentrations * 10^6
[(a) Species transport model; (b)DPM model;
color range from 0 to 5]

Figure 2 compares the concentrations of both tracer gas and particles on the floor (z = 0) and on a plane that cuts the source plume (x = 1 m). On both planes, the major patterns of these two types of simulation have an acceptable agreement with each other. The DPM model generally shows coarser spatial variability in the concentration distribution, while the species transport model shows smooth, continuous contours. The white part in the figures indicates an area where concentration exceeds the highest color range. This plume area is slightly bigger in Fig. 2(a) than in Fig. 2(b) in the vicinity of the back wall, along the right edge. The smoother concentration field and the larger plume area in the tracer gas results can be attributed to greater diffusion, which is part physical and part a product of the DPM model. While the effect of gravity acting on 1 μm particles, specifically the second term on the right-hand side of Eq. (2), is not large enough to explain these differences, the particles are less mobile than the gas. The extent, to which the DPM model exaggerates this effect, as seen in the enhanced particle accumulation in the plume region, is investigated in the next section.

TEST OF NUMBER OF TRIES

As mentioned before, the stochastic tracking is employed in the DPM model. Therefore, the number of tries is a significant parameter in DPM simulations. It represents the number of particles tracked in the DPM model. To compare with results of the species transport model, a sufficiently large number of particles need to be tracked.

a)

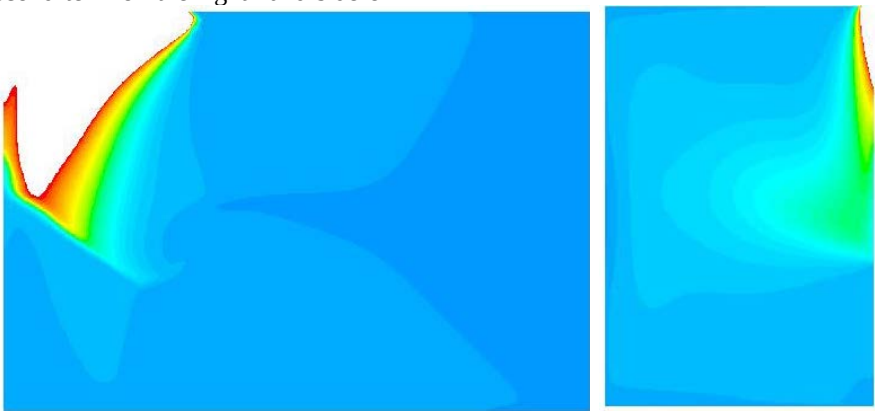

Z=0 x=1

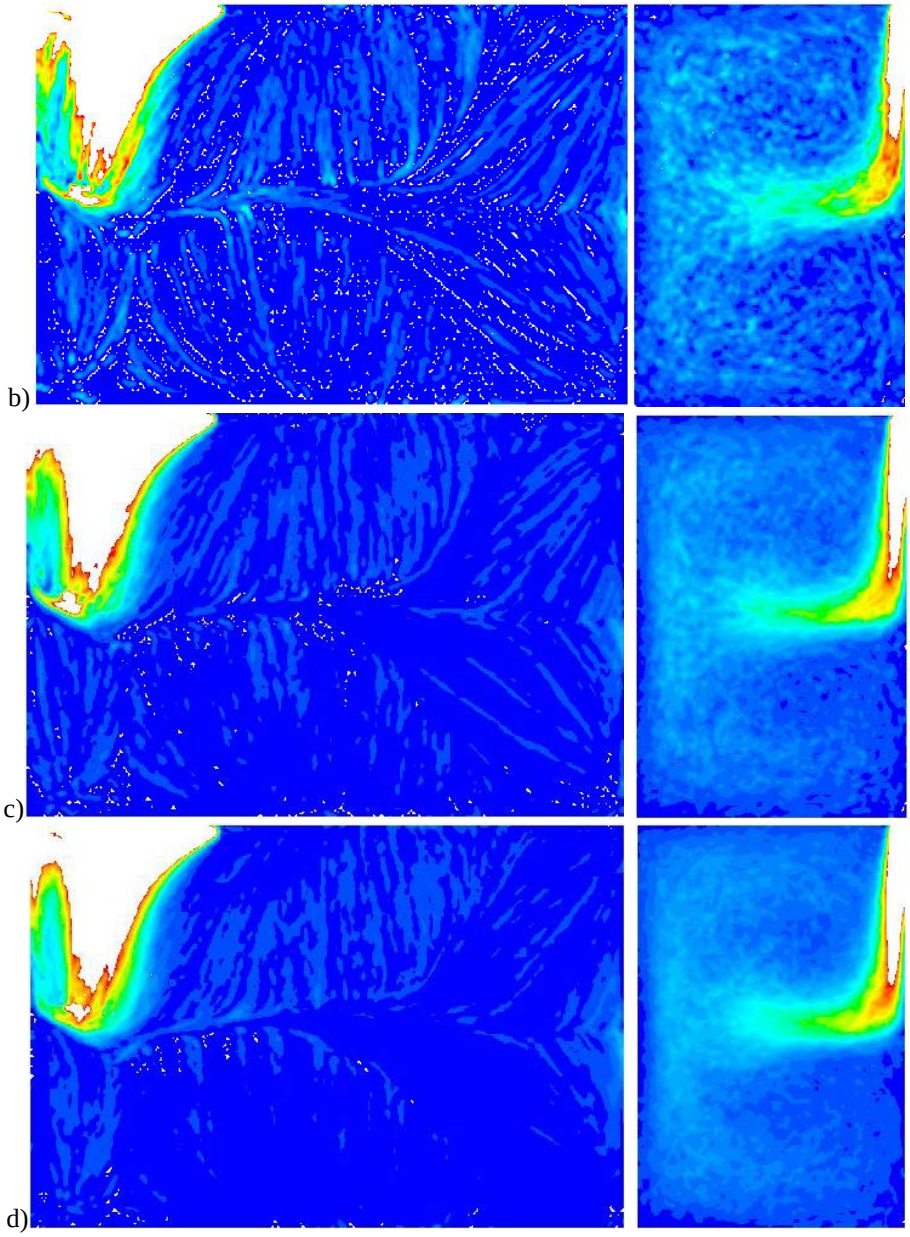

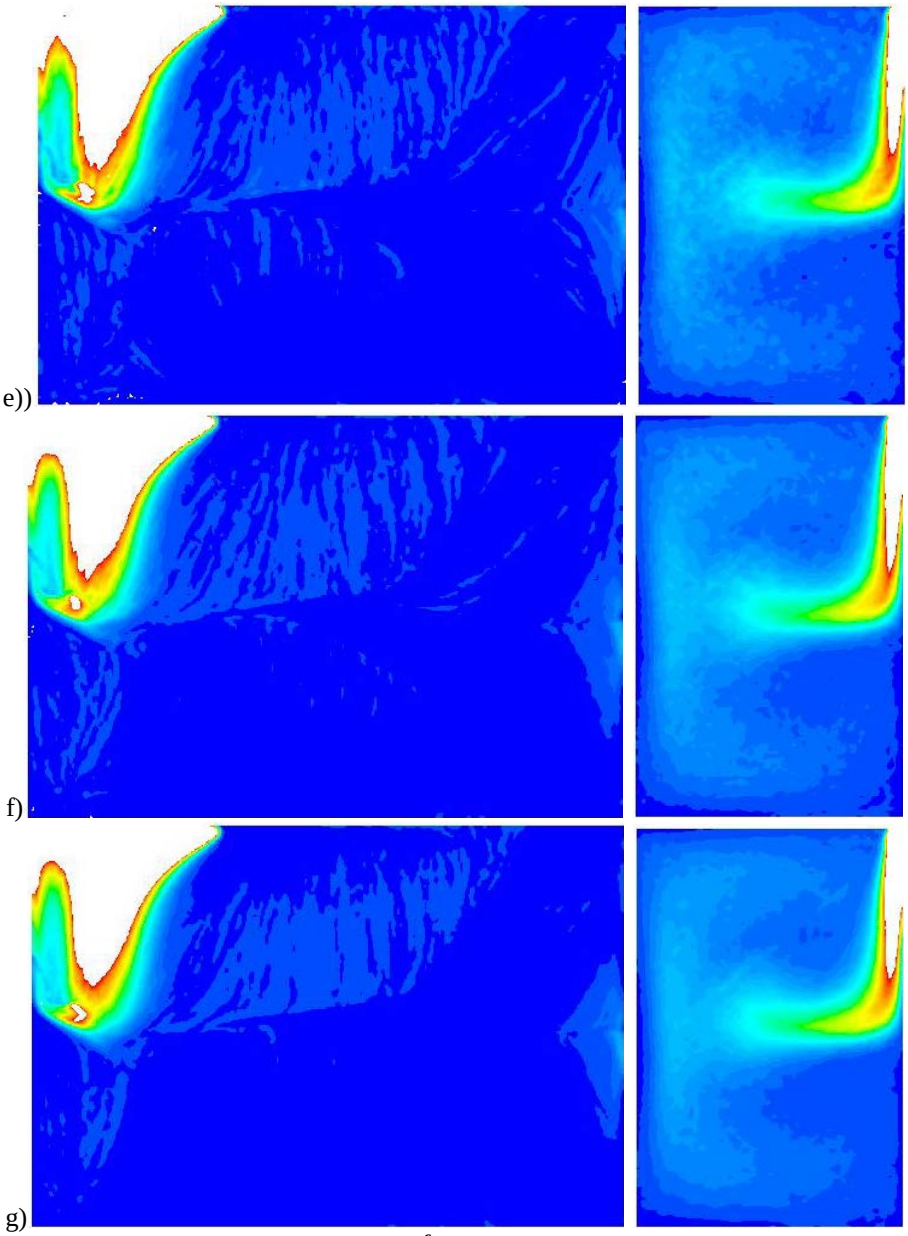

Figure 3- Comparisons of particle mole concentrations * 10^6 from the DPM model with different numbers of tries [left: z = 0 plane, right: x = 1 plane; number of tries: a – Species, b – 16000, c – 64000, d – 128000, e – 256000, f – 512000, g – 1024000; color range from 0 to 5]

If the number of injected particles is less than sufficient, it leads to a very "streaky" contour plot, as in the second row of Fig. 3. Figure 3 also illustrates qualitatively that a number of tries higher than 16,000 does not provide much additional improvement in the discrete phase model result.

COMPARISONS WITH EXPERIMENTAL DATA

In the experiment of [12], the tracer gas concentration in ppm by volume was recorded over time at nine points in the chamber, shown in Fig. 4. The dimensions of the chamber and locations of monitors are only slightly different from that in CFD simulations, which were developed to maximize use of uniform meshing. The numerical results at these nine points have been plotted along with the experimental data in Fig. 5. The experimental results represent 20-minute trials on three consecutive days, while the simulation results have converged to a steady-state solution. Experimental and numerical agreement for the first six locations is acceptable, although values at locations 1 and 4 from the simulation are lower than those from the experiment. However, the experiments show that the concentration at these two locations generally decreased on subsequent days of the experiment. It is possible that the simulation and experimental data might agree better if the

experiment had included additional daily trials. Conversely, the numerical concentration is higher for locations 7, 8 and 9. The spatial variability of the measured concentration was higher than that of the simulated concentration.

In order to compare the experimental results carried out in [12] with the DPM simulation results, the ratio of values between locations 4 and 5, locations 4 and 6, and locations 5 are 6 are compared. The use of these dimensionless ratios removes the issue of comparing the vapor phase volume fraction, e.g. ppm, to the discrete phase mass fraction, e.g. mg/m^3. Figure 6 shows the ratio comparisons among the species simulation, DPM simulation, and tracer gas experiment. While the experiment provides values for each of three days, the averaged value is shown in the figure. It is apparent that the species simulation and DPM simulations with higher numbers of tries (more than 16000) achieve good agreement with the experiment. The case with a lower number of tries has not been shown, since the result does not match at all. The DPM simulation with a lower number of tries results in unrealistically high values of the location concentration ratios, location_4/location_5 and location_4/location_6. Interestingly, location 4 was also a trouble spot for vapor phase agreement.

Since DPM is a statistical model, every one of the cases has been run 20 times. In Fig.6, error bars of averaged values for each case are shown also. It is easily observed that with higher number of tries, the error range of the ratio decreases. Finally, this range becomes to be a 'steady' state, which does not change much. This may be a good judgment to determine if the number of tries is big enough for a DPM simulation.

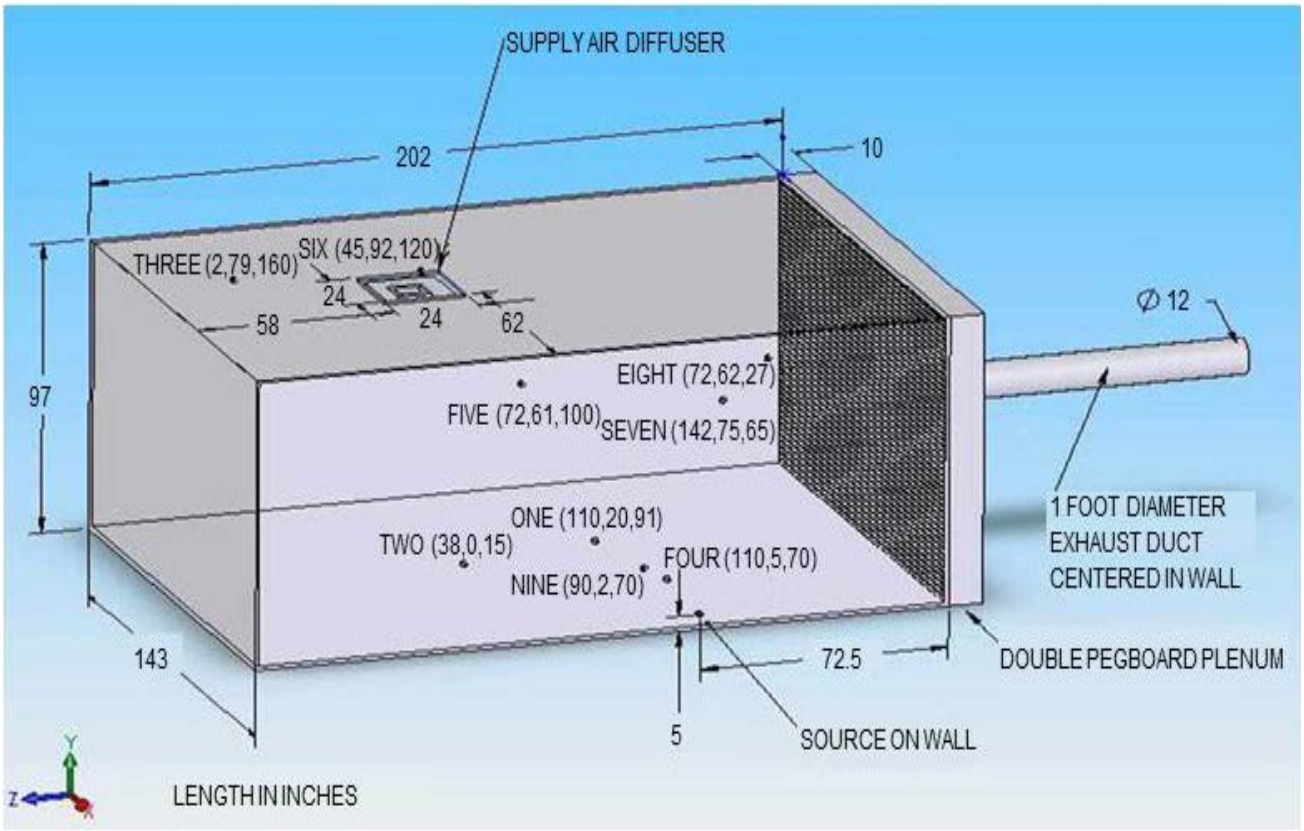

Figure 4 – Nine points in the chamber with recorded ppm data in the experiment (Fig.2 in Shulman et al [12]). Locations of these nine points are corresponding points marked in Fig.1.

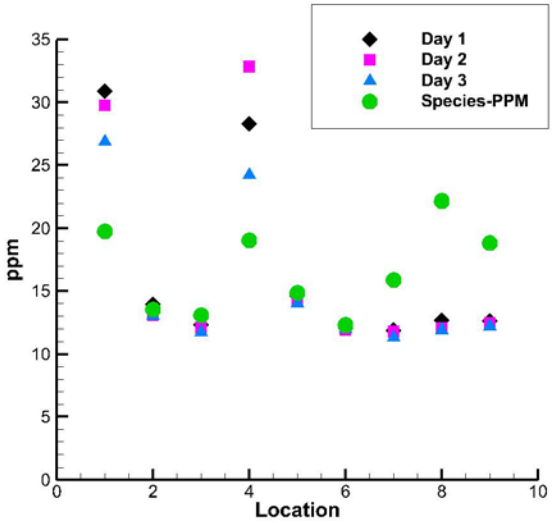

Figure 5 – The comparison of ppm output between the species model and the experiment (Experimental data are from Fig. 8 in [12])

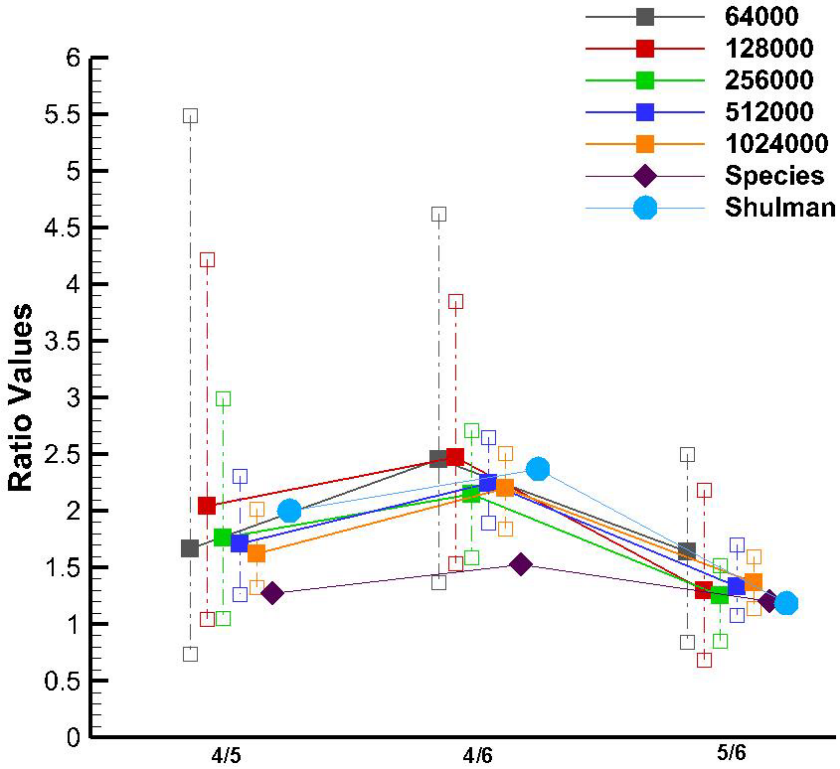

Figure 6 – Ratio comparison among the species simulation, the experiment and DPM simulation with different numbers of tries. Filled rectangle: averaged values; Non-filled ones: error bars of averaged values.

CONCLUSION AND RECOMMENDATIONS

This research has demonstrated the importance of the number of tries in a discrete phase particle model that makes use of the Gaussian eddy interaction concept, as other authors also have found [11]. Without the ability of the random walk approach to effectively fill in the probability space that describes real particle behavior, a simulated particle deposition pattern will be overly convective, lacking adequate opportunity for diffusive transport. Furthermore, without the proper balance between convection and diffusion, the predicted deposition pattern cannot be considered physical. In this work, 16,000 seemed to be a reasonable threshold for an adequate number of

launched particles. This number was achieved here by a combination of particle paths emanating from surface nodes of the source nozzle interior and eddy interaction model tries that created variations of the paths.

ACKNOWLEDGMENTS

The first two authors acknowledge the support of CDC under the contract 212-2010-M-34851.

REFERENCES

[1] Lai, A. C. K., 2002, "Particle deposition indoors: a review," Indoor Air, 12(4), pp. 211-214.
[2] Sun, W., Ji, J., Li, Y. G., and Xie, X. J., 2007, "Dispersion and settling characteristics of evaporating droplets in ventilated room," Build Environ, 42(2), pp. 1011-1017.
[3] Zhang, N., Zheng, Z. C., Glasgow, L., and Braley, B., 2010, "Simulation of particle deposition at the bottom surface in a room-scale chamber with particle injection," Adv Powder Technol, 21(3), pp. 256-267.
[4] Lai, A. C. K., Wang, K., and Chen, F. Z., 2008, "Experimental and numerical study on particle distribution in a two-zone chamber," Atmos Environ, 42(8), pp. 1717-1726.
[5] Zhang, X. Y., and Ahmadi, G., 2005, "Eulerian-Lagrangian simulations of liquid-gas-solid flows in three-phase slurry reactors," Chem Eng Sci, 60(18), pp. 5089-5104.
[6] Lai, A. C. K., and Chen, F. Z., 2007, "Comparison of a new Eulerian model with a modified Lagrangian approach for particle distribution and deposition indoors," Atmos Environ, 41(25), pp. 5249-5256.
[7] Zhang, N., and Zheng, Z. C., 2007, "A collision model for a large number of particles with significantly different sizes," J Phys D Appl Phys, 40(8), pp. 2603-2612.
[8] Morsi, S. A., and Alexande.Aj, 1972, "Investigation of Particle Trajectories in 2-Phase Flow Systems," J Fluid Mech, 55(Sep26), pp. 193-&.
[9] Ounis, H., Ahmadi, G., and Mclaughlin, J. B., 1991, "Brownian Diffusion of Submicrometer Particles in the Viscous Sublayer," J Colloid Interf Sci, 143(1), pp. 266-277.
[10] Moshfegh, A., Shams, M., Ahmadi, G., and Ebrahimi, R., 2010, "A new expression for spherical aerosol drag in slip flow regime," J Aerosol Sci, 41(4), pp. 384-400.
[11] Tian, L., and Ahmadi, G., 2007, "Particle deposition in turbulent duct flows - comparisons of different model predictions," J Aerosol Sci, 38(4), pp. 377-397.
[12] Shulman, S. A., Bennett, J. S., Sieber, W. K., MKatzoff, M. J., Wouhib, A., and Adams, B., 2006, "Estimating Tracer Gas Distribution in a Ventilation Chamber," International Biometric Society - ENAR - ASA Biometrics Section.

Disclaimer: The findings and conclusions in this paper have not been formally disseminated by the National Institute for Occupational Safety and Health and should not be construed to represent any agency determination or policy.